Journal of Engineering Science and Technology
Vol. 18, No. 4 (2023) 1957 - 1972

THIN-LAYER DRYING KINETICS AND QUALITY ATTRIBUTES OF OSMOTIC DEHYDRATED LIME SLICES

THANUTYOT SOMJAI[1],
PARADORN NUTHONG[2], JITTIMON WONGSA[1,3]*

[1]Faculty of Industrial Technology and Management, King Mongkut's University of Technology North Bangkok (Prachinburi Campus), Prachinburi, 25230, Thailand
[2]Faculty of Sciences and Liberal Arts, Rajamangala University of Technology Isan, Nakhonratchasima, 30000, Thailand
[3]Food and Agro-Industry Research Center, Science and Technology Research Institute, King Mongkut's University of Technology North Bangkok, 10800, Bangkok, Thailand
*Corresponding Author: jittimon.w@fitm.kmutnb.ac.th

Abstract

This research investigated the influence of hot air drying (HAD) and direct solar drying (DSD) on the color, texture, and water activity of osmotically dehydrated lime slices. HAD resulted in a faster drying rate and shorter drying time than DSD. The drying curves of the osmotically dehydrated samples under both drying methods were accurately described using the semi-empirical logarithmic model, specifically the Hasibuan and Daud model, which best fit the drying kinetics across all temperatures studied. Heat processes affected the samples' color, water activity, and texture. Increasing the drying temperature significantly enhanced the color values of the dried samples, with HAD at 60°C demonstrating superior color preservation by showing the less total color change. Water activity played a significant role in the samples and influenced the growth rate of different microbes. The drying temperature significantly influenced the hardness of osmotically dehydrated limes. Samples dried at 50°C and 80°C displayed a slight improvement in flavor. Furthermore, the chewiness and cohesiveness of the dried lime slices increased after drying, while the springiness remained consistent. These findings provide valuable insights into the impact of HAD and DSD on osmotically dehydrated lime slices, encompassing aspects such as drying rates, color preservation, water activity, flavor, and texture changes.

Keywords: Hot air drying, Lime slices, Mathematical model, Osmotic dehydration, Quality parameters

1. Introduction

Limes are citrus fruits of various species, and hybrids originate mostly within tropical Southeast Asia and South Asia. In Thailand, the lime-producing area was approximately 17,314.08 hectares in 2020 [1]. Phichit Agricultural Research and Development Center developed a new hybrid lime called "Phichit 1" by crossbreeding the Pan and Nam Hom varieties. Limes are rich sources of vitamin C; they have a sour taste and are often used to accentuate food and beverage flavors. However, Phichit 1 has a thick skin and many seeds, reducing its commercial viability. Citrus fruits have similar anatomical structures, including flavedo, albedo, and carpel segments. Nevertheless, based on the species and variant, the specific components of these structures vary [2]. The primary constituent of citrus peel is albedo, a white, spongy cellulosic tissue. Moreover, due to the presence of associated bioactive components such as flavonoids and vitamin C, which possess antioxidant capabilities, albedo possesses superior quality compared to other sources of dietary fibers [3, 4].

Osmotic dehydration is a pre-drying technique that can effectively decrease energy consumption while improving the quality of food. Three mass transfer processes occur during osmotic dehydration: (1) the leaching of natural solutes from the food, (2) the diffusion of solutes from the osmotic solution into the food, and (3) the diffusion of water from the food material into the surrounding osmotic medium as a result of the concentration gradient between them. It can be used to freeze food without causing undesirable texture changes, lengthen shelf life, lower the freezing load, and somewhat lessen the scent in dried and semi-dried foods [5, 6]. This method can be used as a preliminary phase in the dehydrating process before more advanced drying methods, including convective hot air, freeze drying, and vacuum drying [7].

Drying operations are classical industrialized techniques for preserving agricultural food ingredients or products. Food dehydration is a complex thermal process that entails the simultaneous transfer of heat and mass to eliminate moisture from food [8, 9]. The drying process and time are critical parameters for high-quality dried food products. Direct solar drying (DSD) is used to maximize solar radiation and improve solar drying efficiency over sun/natural drying. [10]. The use of solar dryer (DSD) to generate acceptable the 'Violet de Galmi' onion has also been reported [11]. For designing and operating dryers, as well as upgrading existing drying systems, simulation-based studies are imperative. Consequently, Chandan et al. [9] has recently investigated the drying characteristics or behaviors of diverse food components, such as fruits and vegetables, employing various drying procedures. A model or system with such characteristics is constructed by considering the interaction between time and one or more geographical variables, which serves as the basis for determining its dependent variables. Using the response engineering method (REA), mathematical modeling of convective and intermittent drying [12, 13]. For drying processes, a distributed element model addresses simultaneous mass and heat transmission. Various mathematical models, including the Page model, Henderson and Pabis model, logarithmic model, Singh et al. model, Aghabashlo model, Hasibuan and Daud model, and Simplified Fick's Diffusion model, were utilized to characterize the thin-layer drying curves of a variety of agricultural and food products [14].

This research aims to investigate the drying characteristics and the kinetics of osmotically dehydrated lime slices in DSD and HAD conditions. Additionally, the study aims to model the drying characteristics and kinetics using well-established mathematical drying models, considering the influence of drying temperature on various quality attributes, including color, texture, and water activity (a_w).

2. Materials and methods

2.1. Experimental procedure

2.1.1. Osmotic dehydration (OD)

Fresh limes (*Citrus aurantiifolia* (Christm.) Swingle cv. Pan Phichit) were acquired from a nearby wholesale market. The limes were thoroughly washed, zested, and sliced into 2-3 mm thickness, with the measurements taken manually using a digital caliper. As a pretreatment, the lime slice samples were placed in a glass bottle and immersed in a 27% (w/v) NaCl solution for a duration of 24 hours at room temperature. Following the pretreatment, the samples underwent OD for a period of 3 days. On day 1, the lime slice samples were placed in a 45° Brix osmotic solution containing inverted sugar syrup. The fruit-to-solution ratio was set at 2:3, and the samples were kept at 70°C for 24 h. On day 2, the samples were relocated to a 50° Brix osmotic solution, also containing inverted sugar syrup. The ratio was adjusted to 2:2, and the samples were maintained at 70°C for 24 h. Finally, on day 3, the samples were transferred to a 55° Brix osmotic solution comprising inverted sugar syrup. The was set at 1:2, and the samples were subjected to 70°C for 24 h. [15]. We performed experiments in triplicate. For the purpose of determining the moisture content (M), a sample weighing 2-5 grams was placed in an aluminum container and dehydrated in an oven (Binder, Germany) at 103°C for 72 h, following the guidelines specified by the AOAC [16]. The initial moisture content of the samples varied from 150% to 156% on a dry basis. The values of moisture content on a dry basis (%db) were calculated using the following Eq. (1):

$$M = \left(\frac{W_i - W_d}{W_d}\right) x100 \quad (1)$$

where M is the initial moisture content OD on a dry basis (%db.), W_i is the wet weight of the sample in grams, and W_d is the dry weight of the sample in grams.

2.1.2. Hot air drying (HAD)

HAD was conducted applying a laboratory cabinet dryer, as depicted in Fig. 1(a). The dryer's internal temperature and relative humidity were measured using temperature and relative humidity sensors (Digicon HT-770, Japan). Drying was conducted at temperatures of 50°C, 60°C, 70°C, and 80°C [6]. Once the dryer reached a steady state, the OD samples were placed on a plate positioned on a grill for drying. At regular intervals, the samples were removed, weighed, and then returned to the dryer. The weighing intervals were set at 15 min intervals for the first hour, 30 min intervals for the subsequent hour, and 2 h intervals thereafter. The moisture loss was determined by weighing the plate with a digital balance (AMPUT Electronic Scale, China) with a measurement accuracy of 0.01g. Subsequently, the samples were dried in an oven until they reached a final moisture content of 40%–42% on a dry basis.

2.1.3. Direct solar drying (DSD)

A direct solar drier was used for DSD was shown in Fig. 1(b). In a greenhouse solar drier, DSD was performed for 2 days in the cool to cold season with windy conditions (average temperature of 36.7°C). The OD samples were placed under direct sunlight. PT-100 sensor thermocouples with 0.5°C precision was applied to monitor the drying temperature at the drying container and its exit at regular intervals. Daily, between 9 a.m. and 3.5 p.m., the samples were weighed at 1h intervals [17]. The plate was weighed using a digital balance (AMPUT Electronic Scale, China) with 0.01g measurement accuracy to calculate the moisture loss. Each day, the samples were weighed, and weights recorded after the drying time (DT). Afterward, the samples were baked in an oven until they were completely dry [16]. After drying, the samples were maintained in a desiccator until the temperature of the surrounding air was attained.

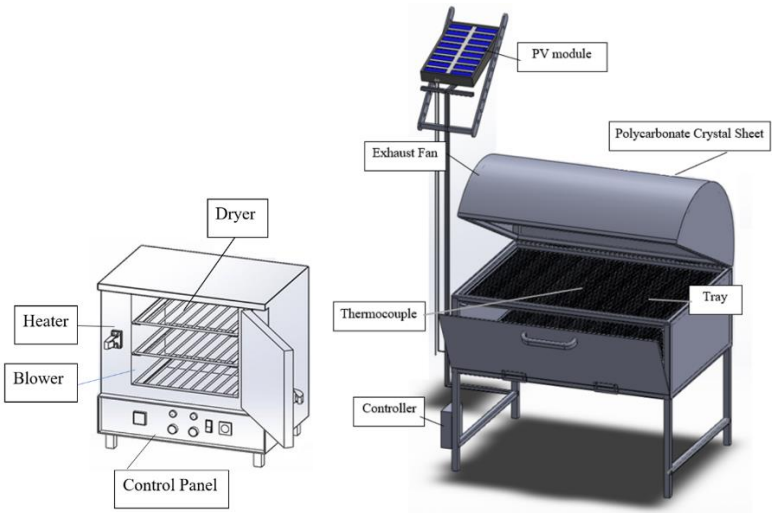

(a) Hot air dryer. **(b) Direct solar dryer.**

Fig. 1. Schematic diagram of dryer.

2.2. Mathematic modeling

2.2.1. Drying Rate (DR)

The drying rate is a measure of moisture loss determined by dividing the moisture content of materials (% dry basis) at two consecutive times by the time gap [18]. The DR can be calculated as follows Eq. (2):

$$DR = \frac{M_t - M_{t+dt}}{dt} \quad (2)$$

where DR has the unit of % dry basis /min, M_t is moisture content (% db.) of sample at time t, M_{t+dt} moisture content (% db.) of sample at time t + dt and *dt* denotes the drying time (min).

2.2.2. Fitting of Thin-Layer Drying Curves

Drying kinetics refers to the rate at which the M changes during the drying process. The typical drying kinetics exhibit an initial drying phase, followed by a phase of constant DR, and finally a phase of decreasing drying rate as the process progresses. This drying process can be illustrated by constructing a drying curve, which can be utilized to predict drying conditions based on the relationship between M and time [19]. To fit data for the necessary empirical models, the dry basis (% db.) M of the samples is converted to a dimensionless moisture ratio ($MR = \frac{M_t - M_{eq}}{M_o - M_{eq}}$) and the drying kinetic curve is generated by plotting MR versus time. The MR can be simplified to M_t/M_0 because M_{eq} is relatively small and as compared to M_t ($M_{eq} << M_t$) and M_0($M_{eq} << M_o$) [20].

To evaluate the drying kinetics and estimate the MR based on drying time, the MRs and drying times (DTs) were fitted to eight widely employed thin layer drying models, which are presented in Table 1. The specific constants for each model were determined using nonlinear regression techniques. During data fitting for modelling purposes, it was presumed that all samples had a similar initial M and that there was no loss of heat through the dryer insulation. Additionally, any internal temperature gradients within the samples, variations in drying air humidity, heat transfer within the material, and volume contraction rate during drying were considered negligible.

Table 1. Thin-layer drying mathematical models.

Model name	Equation	References
Newton	MR = $\exp(-kt)$	[21]
Page	MR = $\exp(-kt^n)$	[22]
Henderson and Pabis	MR = $a\exp(-kt)$	[14]
Logarithmic	MR = $a\exp(-kt)$ +c	[20]
Singh et al.	MR = exp(-*kt*)-akt	[14]
Aghabashlo Model	MR = exp-($\frac{k_1 t}{1+k_0 t}$)	[14]
Hasibuan and Daud	MR = 1-$at^n\exp(-kt^n)$	[14]
Simplified Fick's Diffusion	MR = $a\exp(-kt)$ +c	[14]

The root-mean-square error (RMSE) was utilized for quantify the disparity between the experimental results and the values estimated by the models. The model exhibiting the highest correlation coefficient (R^2), reduced chi-square (χ^2), and lowest RMSE [23] was determined to have the best fit.

$$R^2 = 1 - \frac{\sum_{i=1}^{N}\left(MR_{exp,i} - MR_{pre,i}\right)^2}{\sum_{i=1}^{N}\left(\overline{MR}_{exp,i} - MR_{pre,i}\right)^2} \quad (3)$$

$$\chi^2 = \frac{\sum_{i=1}^{N}\left(MR_{exp,i} - MR_{pre,i}\right)^2}{N-n} \quad (4)$$

$$RMSE = \frac{1}{N}\left[\sum_{i=1}^{N}\left(MR_{exp,i} - MR_{pre,i}\right)^2\right]^{1/2} \quad (5)$$

2.2.3. Calculation of effective diffusivity

Fick's diffusion equation might be used to characterize the period of decreasing drying rate for the characteristics of biological products [24]. While this equation

may not precisely fit the experimental data, it offers an approximate means of making a quantitative comparison between different products in terms of moisture transfer. This is because it can provide an estimation of the average diffusion coefficient throughout the drying process. Crank's [25] approach has been applied to a variety of typically shaped objects, including rectangular, cylindrical, and spherical items. The MR can be expressed in a logarithmic form for a lengthy drying period as follows Eq. (6):

$$\frac{M_t - M_{eq}}{M_o - M_{eq}} = \frac{8}{\pi^2} \sum_{n=0}^{\infty} \frac{1}{(2n+1)^2} exp\left(-\frac{(2n+1)^2 \pi^2 D_{eff} t}{4L_o^2}\right) \quad (6)$$

where D_{eff} denotes the effective diffusivity, L_o denotes half of the thickness of samples, and t denotes the corresponding DT. Equation (7) was simplified to only the first term expressed in a logarithmic form as follows:

$$InMR = In\frac{8}{\pi^2} - \frac{\pi^2 D_{eff} t}{4L_o^2} \quad (7)$$

The effective diffusivity can be determined by plotting the ln(MR) against the DT, This plot will yield a straight line with a slope of $\frac{\pi^2 D_{eff}}{4L_o^2}$.

2.2.4. Calculation of activation energy

The activation energy serves as an indicator of energy required for removing water from a product. An Arrhenius-type relationship can be utilized to describe the effective diffusivity, considering the significant impact of temperature on diffusivity [26], as follows Eq. (8):

$$D_{eff} = D_0 \exp\left(-\frac{E_a}{RT}\right), \quad (8)$$

where D_0 denotes the pre-exponential factor of the Arrhenius equation (m^2/h), E_a represents the activation energy (kJ/mol), R represents the universal gas constant (8.314 kJ/kmol K), and T represents the absolute temperature (K).

2.3. Physicochemical analyses

2.3.1. Color

To determine the surface color of both fresh and dried lime slice samples, two measurements were taken on the two symmetrical faces with a Minolta Chroma Meter II Reflectance CR-300 colorimeter (Minolta, Osaka, Japan). For each temperature, 10 sets of color measurements were individually performed. The standard deviation was used to express the average results. The CIELAB color values (L^*, a^*, and b^*) were calculated, and the average values were determined for all samples.

The polar or cylindrical coordinates - hue angle and chroma—as described by Eqs. (9) and (10), may be calculated using these Cartesian coordinates [27] as follows:

$$Hue\ angle = tan^{-1}\frac{b^*}{a^*} \quad (9)$$

$$Chroma = \sqrt{(a*)^2 + (b*)^2} \quad (10)$$

In Eq. (10), the total color change (ΔE) was employed to assess the overall color difference among a dehydrated sample and the reference product.

$$\Delta E = \sqrt{(L_o^* - L^*)^2 + (a_o^* - a^*)^2 + (b_o^* - b^*)^2} \quad (11)$$

where L_o^*, a_o^*, and b_o^* denote the color values of osmotically dehydrated samples, and L^*, a^*, and b^* denote the color values of the dried samples.

2.3.2. Texture

The texture of sample was assessed using the texture analyzer (CT3 Texture Analyzer, BROOKFIELD, USA) with fixture base table and cylindrical probe in Texture Profile Analysis (TPA) compression mode. The trigger force was 0.1 N, and the pre-test, test, and post-test speeds were 1, 10, and 1 mm/s, respectively. For data analyses, five samples were measured, and the average force was employed. Hardness, cohesiveness, springiness, and chewiness were the quality criteria assessed [28].

2.3.3. Water activity

The water activity (a_w) of the samples was measured by a water activity meter (LabTouch-AW "BASIC"; Novasina, Switzerland). To determine the water activity, 2 g samples were maintained at 25°C ± 0.1°C until equilibrium was established. The experiment was repeated three times of measurement were used. According to the Thai Community Product Standard [29], dried fruits and vegetables must satisfy $a_w < 0.6$.

2.4. Statistical analyses

An analysis of variance (ANOVA) was conducted on the experimental data for color, water activity, and sensory rating using IBM SPSS Statistics Version 26.0. Multiple comparisons were performed using Duncan's test with a significance level of 95% ($p < 0.05$) to determine the differences between mean values.

3. Results and Discussion

3.1. Drying characteristics

3.1.1. Hot air drying kinetics

The drying kinetics of osmotically dehydrated samples determined under HAD for initial M varied from 147% to 156% dry basis (kg water/kg dry matter). Figure 2(a) shows the drying curve for the MR of osmotically dehydrated lime slices samples over time when dried at 50°C, 60°C, 70°C, and 80°C. The different drying times used in this study were determined to be 10, 8.5, 5, and 3.5 h, respectively. The drying time at 50°C was 0.65 times longer than that at 80°C. The drying temperature significantly influenced the DT. A higher temperature of the drying medium requires more heat power and facilitates greater air movement, resulting in a reduced drying time [21, 30]. The samples were dried until their weight did not change with time, corresponding to a final M of approximately 40%–42% dry basis. The relationship between the MR and DT curves of osmotically dehydrated lime slices samples at different drying temperatures showed that the higher the temperature, the shorter the drying time, whereas the MR values of osmotically dehydrated lime slices samples were the same during the drying process.

3.1.2. Direct solar drying kinetics

Figure 2(b) depicts the drying curve for osmotically dehydrated samples, where the M is highest at the start of the process and begins to decrease shortly after drying begins. The moisture loss is more noticeable in the early stages and becomes less significant as the process progresses. As the rate of moisture loss is higher during this phase, the amount of free water present at the start is critical. As the drying process progresses, the amount of available free water reduces fast, and the removal of bound water occurs in the late stages, requiring enormous energy and is thus a slow process. Several researchers [21] have reported this as a common drying behaviour for agricultural products. Lime slices with an initial moisture level of 147%–156% dry basis were dried to an M of 40%–42% dry basis. DSD generated a product with an M within the acceptable M for dried produce stability, but the approach is unreliable because it depends on natural meteorological conditions that are difficult to manage. Figure 3 compares the temperature created inside the solar dryer with the ambient temperature during the drying period. The temperature of the dryer varied within 40.17°C ± 5.97°C, and it was discovered that the temperature created in the dryer was always higher than the ambient temperature. As the sun reaches its highest point in the sky, the temperature in the dryer rises drastically between 12 noon and 1 p.m. At this point, the angle of insolation was closest to 90°, resulting in intense sun radiation [21]. The recommended drying temperature for most food products is 60°C-70°C.

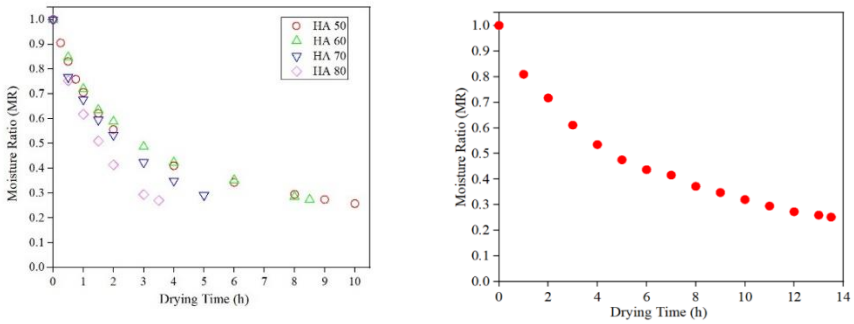

(a) at HAD. **(b) at DSD.**

Fig. 2. Drying kinetics curve of osmotically dehydrated lime slices.

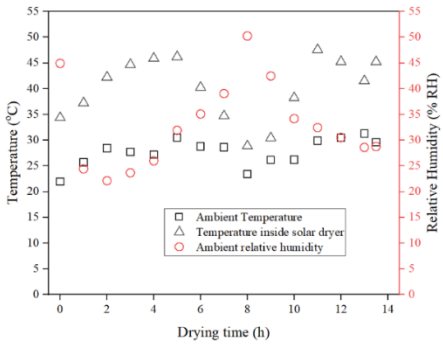

Fig. 3. Comparison of ambient, inside solar dryer temperatures and ambient relative humidity with respect to DT.

These results suggested that the effect of air temperature is reflected with the DR for osmotically dehydrated lime slices. Further, as observed from the curves, the correlated slope indicates that the DR of lime slices is fast in the early and middle stages and tends to slow down gradually in the late stages (Fig. 4(a)). The osmotically dehydrated lime slices drying curves at various temperatures revealed a diminishing rate as the item dried more and approached its equilibrium moisture content. The drying characteristic curves depict the relationship between the drying rate profile and the moisture content on a dry basis. Figure 4(b) makes this point evident, and drying rates become pretty low at low moisture content. The individual material and drying conditions will, of course, affect how precisely these curves are detailed. The drying at this stage is provided by external heat transfer. Food transfers moisture while drying. A moisture concentration gradient acts as the driving force behind moisture transfer by diffusion. Ventilation drying can typically be separated into two drying phases: a constant-rate phase where the drying rate is constant, and a falling-rate phase where the drying rate gradually declines as drying advances. During the falling rate period, drying is governed by the resistance to internal mass transfer. The shape of the drying rate curve is influenced by the characteristics of the material being dried and the type of mass transfer that is dominant. No constant drying period is observed for solids where the mass transfer is completely controlled by internal diffusion or completely hygroscopic biological solids [31]. When a water activity gradient exists, water is evaporated off the surface of the item being dried through convective drying. The higher the temperature, especially at the start of the process, the faster the rate of drying. The drying rate of samples was calculated by equation (2). Drying rates ranged from 0.195% dry basis /min for experiments at 50ºC, 0.218 % dry basis /min for experiments at 60ºC, 0.348 % dry basis /min for experiments at 70ºC, and 0.520 % dry basis/min for experiments at 80ºC. Higher drying rates are correlated with higher air temperatures, and variations in drying rates for each of the examined temperature levels decrease as the water content of the item being dried decreases. The drying rate in the direct passive solar dryer was 0.145 % dry basis /min.

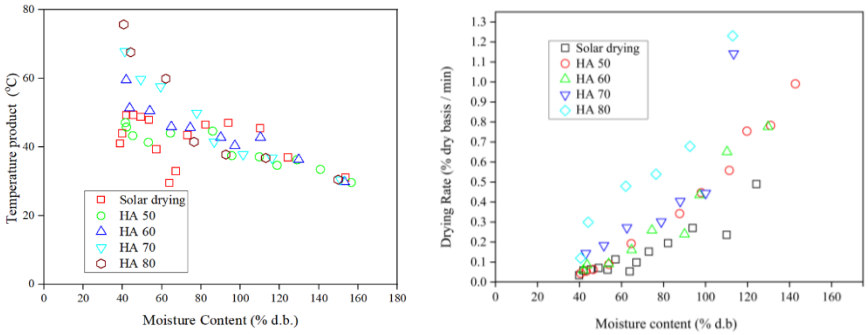

(a) Temperature with the M curve. **(b) DR with M curve.**

Fig. 4. DR and Temperature products with the dry basis of M of the curve.

3.2. Effective moisture diffusivity

As a result of the falling rate interval, the results reveal that the internal mass transfer resistance influences the drying time. Fick's diffusion equation was used

to adapt the experimental drying curves obtained under the solar and hot air temperatures (Eq. 7). The effective diffusivity of the osmotically dehydrated lime slices in the present solar and hot air dryers was calculated by plotting ln(MR) against drying time [Fig. 2], where the slope of the straight line gives the effective diffusivity. The effective moisture diffusivity values were summarized in Table 2. The average effective diffusivities of osmotically dehydrated samples HAD process ranged from 5.461 $\times 10^{-8}$ to 12.702 $\times 10^{-8}$ m^2/h for HAD and 3.786 $\times 10^{-8}$ m^2/h for DSD, respectively. These values are within the general range of 10^{-9} to 10^{-11} m^2/s for the drying of food materials [31]. The apparent activation energy (E_a) values were calculated from Equation 8, which were 31775.1 kJ/mol. The values of D_{eff} increased with temperature, as expected. When the initial M was the same, the average effective diffusivities in HAD were more significant than those in DSD, indicating that HAD had better mass transfer efficiency than DSD. The results provide valuable insights into the mechanisms of moisture transfer and have practical implications for optimizing operating conditions in the drying industry of osmotically dehydrated lime slices.

Table 2. Effective moisture diffusivities of samples dried with HAD and DSD.

Condition	Moisture Diffusivity(m^2/h)	D_0 (m^2/h)	E_a (kJ/mol)
Hot air (50°C)	5.461×10^{-8}		
Hot air (60°C)	5.782×10^{-8}	6.153×10^{-3}	31775.1
Hot air (70°C)	8.337×10^{-8}		
Hot air (80°C)	12.702×10^{-8}		
DSD	3.786×10^{-8}		

3.3. Mathematical modeling

The drying kinetics of many agricultural and food commodities can be anticipated using thin-layer drying models. The statistical parameters and anticipated model parameters for the empirical equations used to forecast the water content as a function of DT. The highest R^2 and lowest RMSE and χ^2 values were found in the Hasibuan and Daud model. Consequently, the Hasibuan and Daud model was employed to characterize the thin-layer drying characteristics of osmotically dehydrated lime slices. The statistical findings for the drying of samples are summarized in Table 3. Under various drying conditions, the experimental and calculated MR distributions are presented. The Hasibuan and Daud model could forecast M evolution for osmotically dehydrated lime slices at each drying temperature with a high degree of accuracy [32].

Table 3. Statistical analysis results for HAD and DSD models.

Model	Condition	Constant	R^2	RMSE	X^2
Newton	HAD 50°C	k = 0.200419	0.91970	0.03655	0.00200
	HAD 60°C	k = 0.207569	0.93399	0.02951	0.00131
	HAD 70°C	k = 0.297052	0.95735	0.02142	0.00069
	HAD 80°C	k = 0.432176	0.98526	0.01298	0.00025
	Direct solar	k = 0.124985	0.95856	0.02088	0.00065
Page	HAD 50°C	k = 0.343112, n = 0.626502	0.99148	0.00919	0.00012
	HAD 60°C	k = 0.331518, n = 0.654227	0.99492	0.00667	0.00007
	HAD 70°C	k = 0.396585, n = 0.695018	0.99893	0.00292	0.00001
	HAD 80°C	k = 0.490807, n = 0.806227	0.99904	0.00307	0.00001
	Direct solar	k = 0.224277, n = 0.708356	0.99755	0.00433	0.00003

Henderson and Pabis	HAD 50°C	k = 0.158156, a = 0.885112	0.93842	0.02590	0.00100
	HAD 60°C	k = 0.172377, a = 0.901078	0.94623	0.02232	0.00075
	HAD 70°C	k = 0.260878, a = 0.925861	0.96903	0.01590	0.00038
	HAD 80°C	k = 0.408837, a = 0.962762	0.98815	0.01094	0.00018
	Direct solar	k = 0.110305, a = 0.911909	0.96919	0.01566	0.00037
Logarithmic	HAD 50°C	k = 0.461831, a = 0.707392, c = 0.274000	0.99643	0.00612	0.00005
	HAD 60°C	k = 0.413312, a = 0.713419, c = 0.269971	0.99533	0.00643	0.00006
	HAD 70°C	k = 0.501789, a = 0.720933, c = 0.251034	0.98991	0.00892	0.00012
	HAD 80°C	k = 0.623773, a = 0.813219, c = 0.178403	0.99820	0.00419	0.00003
	Direct solar	k =0.214029, a = 0.755427, c = 0.223592	0.99621	0.00539	0.00004
Singh et al.	HAD 50°C	k = 0.339936, a = -0.07817	0.98695	0.01230	0.00022
	HAD 60°C	k = 0.313044, a = -0.085693	0.98929	0.01012	0.00015
	HAD 70°C	k = 0.416726, a = -0.091573	0.98502	0.01141	0.00020
	HAD 80°C	k = 0.542339, a = -0.064628	0.99766	0.00485	0.00004
	Direct solar	k = 0.175509, a = -0.075783	0.99260	0.00781	0.00009
Aghabashlo Model	HAD 50°C	K_1 = 0.418072, K_0 = 0.214778	0.99974	0.00163	0.000004
	HAD 60°C	K_1 = 0.368236, K_0 = 0.173588	0.99881	0.00326	0.00002
	HAD 70°C	K_1 = 0.463011, K_0 = 0.195002	0.99286	0.00766	0.00009
	HAD 80°C	K_1 = 0.561515, K_0 = 0.140113	0.99863	0.00368	0.00002
	Direct solar	K_1 = 0.199113, K_0 = 0.073244	0.99826	0.00368	0.00002
Hasbuan And Daud	HAD 50°C	a =0.341309, n = 0.745576, k = 0.172122	0.99782	0.00475	0.00003
	HAD 60°C	a =0.321251, n = 0.751860, k = 0.160660	0.99788	0.00432	0.00003
	HAD 70°C	a =0.368144, n = 0.593828, k = 0.114131	0.99958	0.00183	0.00001
	HAD 80°C	a =0.481967, n = 0.828044, k = 0.218183	0.99932	0.00258	0.00001
	Direct solar	a =0.209431, n = 0.760185, k = 0.098224	0.99853	0.00336	0.00002
Simplified Fick's Diffusion	HAD 50°C	a =0.707392, k = 0.461831, c = 0.274000	0.99643	0.00612	0.00005
	HAD 60°C	a =0.713419, k = 0.413312, c = 0.269971	0.99533	0.00643	0.00006
	HAD 70°C	a =0.720953, k = 0.501798, c = 0.251034	0.98991	0.00892	0.00012
	HAD 80°C	a =0.813219, k = 0.623773, c = 0.178403	0.99820	0.00419	0.00003
	Direct solar	a =0.755427, k = 0.214029, c = 0.223592	0.99621	0.00539	0.00004

3.4. Color

Table 4 presents the average values of the color parameters for fresh, osmotically dehydrated, and dried specimens. L^* denotes the brightness, a^* the redness, b^* the yellowness, chroma, hue angle and total color difference (ΔE). The fresh lime slices had L^*, a^*, and b^* values of 48.48, −1.79, and 15.30, respectively. The osmotically dehydrated lime slices had a light-yellow color, with decreased L^* (20.73) but increased a^* (−1.09) and b^* (22.89). However, there were no significant differences in L^* values when the temperature was increased from 70°C to 80°C and DSD was used. The drying conditions affected the a^* and b^* parameters, that is, temperature and time, respectively. The dehydrated samples' a^* and b^* values increased after the drying process. Hence, increasing the air temperature increased the rate of color

degradation because of the high level of energy transfer to the lime slices [33], attributable to the degradation of red pigments or their conversion into dark pigments due to the Maillard reaction [34]. Low values of overall color change (ΔE), which plays an essential role in consumer acceptance, may be associated with the best quality of dried lime slices. ΔE had a minimum value of 7.23 for samples dried at 60°C. The chroma and hue angle data revealed color stability for the samples dried at 50°C–60°C and an increase in the color intensity for samples dried at 70°C–80°C, shifting toward the somewhat yellow zone. The prolonged exposure to the drying process at low temperatures and the occurrence of non-enzymatic browning reactions throughout the process may explain these results, as temperature and DT are crucial factors in color degradation [35].

Table 4. Color of dried limes.

Sample	L^*	a^*	b^*	ΔE	Chroma	Hue angle
Fresh limes	48.48^{d}	-1.79^{a}	15.30^{a}	-	15.40^{a}	96.68^{a}
OD limes	20.73^{a}	-1.09^{b}	22.89^{b}	-	22.92^{b}	92.73^{a}
HAD 50	29.05^{b}	0.17^{c}	19.50^{b}	9.07	19.50^{b}	$89.50^{a,b}$
HAD 60	27.02^{b}	2.18^{e}	21.49^{b}	7.23	21.60^{b}	84.21^{c}
HAD 70	35.71^{c}	2.44^{e}	26.41^{c}	15.79	26.52^{c}	84.72^{c}
HAD 80	32.46^{c}	3.02^{f}	29.70^{c}	14.17	29.85^{c}	84.19^{c}
DSD	34.68^{c}	1.45^{d}	19.49^{b}	14.58	19.54^{b}	$85.75^{b,c}$

^{a,b,c,d,e,f} Means at the same row without the same superscript are significantly different ($p < 0.05$).

3.5. Water activity

Water activity (a_w) is used by food producers to develop shelf-stable products. Low water activity also helps keep product quality high and extend shelf life. This study indicated that the M of osmotically dehydrated and dried lime slices was 40%–42%. Table 5 shows that water activity was much greater in fresh and osmotically dehydrated limes (before drying) than in other samples. There was no difference in water activity between hot air-dried (60°C–80°C) and solar-dried samples ($p > 0.05$), indicating that the water activity was 0.47–0.52, as required by Thai Community Product Standards [29].

3.6. Texture

Table 5 shows the estimated values of the textural qualities obtained from the texture analyzer. The force exerted by mastication when eating is related to the parameter hardness. Fresh lime slices have a higher hardness value than osmotic lime slices, possibly due to the use of a high-temperature inverted sugar syrup solution in the osmotic process, destroying the tissue structure and resulting in a softer texture. However, HAD and DSD drying processes increase the lime slices' hardness, possibly due to the evaporation of moisture. The creation of a sugar coating on the surface of the slices may be the cause of the samples treated with sucrose having greater hardness ratings [36]. The cohesiveness of osmotically dehydrated samples remained essentially constant after drying, with only a minor increase, showing that fresh and dried samples have similar internal bonding strengths. Cohesiveness increased from the fresh to the dried condition, as well as with increasing drying temperature. The springiness of the samples dried at higher temperatures, which is a measure of height recovery after compression during

mastication, was higher. Based on the springiness values, it is also reasonable to conclude that drying (convective air drying) did not significantly affect the ability of the osmotically dehydrated lime slices to return to their original shape after deformation. A notable exception was the solar-dried product, which had a lower springiness score than the other cases. Chewiness increased dramatically with drying temperature, which matched the hardness fluctuation in a previous study [37]. Comparing the two drying methods revealed that the texture of lime slices dried at 80°C was more susceptible to HAD, especially at the maximal temperature, than DSD. The results indicated that the texture of dried samples was more sensitive to HAD, especially at the maximum temperature [28].

Table 5. Water activity and textural attributes and water activity of dried limes.

Sample	Water activity	Hardness (N)	Cohesiveness	Springiness (%)	Chewiness (N)
Fresh limes	0.89^{d}	22.43^{c}	0.34^{a}	$1.62^{a,b}$	13.20^{b}
OD limes	0.80^{c}	7.46^{a}	0.32^{a}	1.43^{a}	3.29^{a}
HAD 50	0.52^{b}	$11.73^{a,b}$	0.46^{b}	$2.21^{b,c}$	10.00^{b}
HAD 60	0.47^{a}	$9.23^{a,b}$	0.53^{b}	2.31^{c}	11.57^{b}
HAD 70	0.48^{a}	$10.20^{a,b}$	0.52^{b}	2.51^{c}	$16.78^{b,c}$
HAD 80	0.48^{a}	13.72^{b}	0.73^{c}	$2.63^{c,d}$	26.06^{d}
DSD	0.48^{a}	$11.29^{a,b}$	0.47^{b}	1.90^{b}	12.23^{b}

^{a,b,c,d} Means at the same row without the same superscript are significantly different ($p < 0.05$).

4. Conclusions

The drying features and kinetics of osmotically dehydrated lime slices were explored in relation to the drying technique (DSD and HAD) and drying temperature (50°C–80°C). The findings revealed that the drying technique and drying temperature significantly influenced the DR and hence the DT. The osmotically dehydrated lime slices had an initial M of 147%–156% (d.b.), and they were then dried in an oven until they had a final M of 40%–42% (d.b.). Under DSD and HAD conditions, lime slices dried properly in 3.5–10 and 13 h, respectively. Regardless of the drying process, all samples dried at a decreasing pace, with no constant rate period. The experimental drying curves were fitted to mathematical drying models. The drying properties, color, texture, and water activity of the samples were studied in relation to the drying temperature. The Hasibuan and Daud model showed the best fit to the experimental data acquired from DSD and HAD, respectively. MR in relation to DT was calculated using a correlation between the model parameters and drying temperature (under HAD). Fick's diffusion equation was used to characterize water transport during drying, and the effective moisture diffusivity was calculated. The DSD value was 3.786×10^{-8} m^2/h, whereas the HAD values ranged from 5.461×10^{-8} to 12.702×10^{-8} m^2/h. Regarding the color, it was possible to conclude that HAD at 60°C improved the color retention of dried lime slices. Water activity was a significant factor in the samples, and the rate at which different microbes grew was influenced by it. Bacteria and mold growth can be prevented if the water activity is reduced to 0.6. Controlling water activity can help detect spoilage while reducing the water activity of lime slices through OD. The hardness of fresh and osmotically dehydrated lime slices differed. Results indicate that increasing the drying temperature significantly increased hardness of

dehydrated lime slices dramatically, and the drying technique affected the dehydrated samples. Further, chewiness was higher in dehydrated samples than in fresh samples, but springiness had the reverse impact. In addition, lowering the drying temperature reduced the chewiness and hardness of the dehydrated product while keeping the cohesiveness and springiness slightly constant.

Acknowledgment

This research was funded by King Mongkut's University of Technology North Bangkok. Contract no. KMUTNB-64-DRIVE-31.

Nomenclatures

MR	Moisture ratio (dimensionless)
R^2	Determination of coefficient
RMSE	Root mean square error

Greek Symbols

χ^2	Reduced chi-square

Abbreviations

DR	Drying Rate
DSD	Direct Solar Drying
DT	Drying Time
HAD	Hot Air Drying
M	Moisture Content
Meq	Equilibrium moisture content
OD	Osmotic Dehydration

References

1. Office of Agricultural Economics.(2020). Lime producing area in Thailand. Ministry of Agriculture and Cooperatives, Thailand. Retrieved May 1, 2022, from https://www.oae.go.th
2. Rivera-Cabrera, F.; Ponce-Valadez, M.; Sánchez, F.; Villegas-Monter, Á.; and Pérez-Flores, L.J. (2009). Acid limes. A review. *Fresh Produce*, 4, 116-122.
3. Benavente-García, O.; Castillo, J.; Marin, F.R.; Ortuño, A.; and Del Río, J.A. (1997). Uses and properties of *Citrus* flavonoids. *Journal of Agriculture and Food Chemistry*, 45(12), 4505-4515.
4. Aleson-Carbonell, L.; Fernández-López, J.; Sayas-Barberá, E.; Sendra, E.; and Pérez-Alvarez, J.A. (2003). Utilization of lemon albedo in dry-cured sausages. *Journal of Food Science*, 68(5), 1826-1830.
5. Solanke, S.; Deshmukh, S.; and Patil, B.N. (2018). Development of osmo-convective drying of sweet orange slices by using different osmotic agents. *International Journal of Chemical Studies*, 6, 838-842.
6. Petrotos, K.B.; and Lazarides, H.N. (2001). Osmotic concentration of liquid foods. *Journal of Food Engineering*, 49(2-3), 201-206.

7. Naknean, A. (2012). Factors affecting mass transfer during osmotic dehydration of fruit, *International Food Research Journal*, 19, 7-18.
8. Afolabi, T.J. (2014). Thin layer drying kinetics and modelling of Okra (*Abelmoschus esculentus* (L.) Moench) slices under natural and forced convective air drying. *Food Science and Quality Management*, 28, 35-50.
9. Chandan, K.; Karim, M.A.; and Mohammad, U.H. Joardder. (2014). Intermittent drying of food products: A critical review. *Journal of Food Engineering*, 121, 48-57.
10. Hii, C.L.; Ong, S.P.; Yap, J.Y.; Putranto, A.; and Mangindaan, D. (2021). Hybrid drying of food and bioproducts: A review. *Drying Technology*, 39(11), 1554-1576.
11. Compaore, A.; Dissa, A.O.; Rogaume, Y.; Putranto, A.; Chen, X.D.; Mangindaan, D.; Zoulalian, A.; Rémond, R.; and Tiendrebeogo, E. (2017). Application of the reaction engineering approach (REA) for modeling of the convective drying of onion. *Drying Technology*, 35(4),500-508.
12. Putranto, A.; Chen, X.D.; Xiao, Z.; and Webley, P.A. (2011). Mathematical modeling of intermittent and convective drying of rice and coffee using the reaction engineering approach (REA). *Journal of Food Engineering*, 105, 638-646.
13. Putranto, A.; Xiao, Z.; Chen, X.D.; and Webley, P.A. (2011). Intermittent drying of mango tissues: implementation of the reaction engineering approach. *Industrial & Engineering Chemistry Research*, 50, 1089-1098.
14. Uwem, E.I.; Innocent, O.O.; and Benjamin, R.E. (2018). Kinetic models for drying techniques - Food materials. *Advances in Chemical Engineering and Science*, 8, 27-48 .
15. Puechkaset. (2020). Osmotic preserving technology of fruit and processing preparation. Retrieved June 1, 2022, from https://www.puechkaset.com
16. AOAC. (1995). *Official method of analysis*. (16th ed.). The association of official analytical chemists. Inc. Arlington, Verginia, USA.
17. Ankit, K.; Kamred, U.S.; Mukesh, K.S.; Alok, K.S.K; Abhishek, K.; and Shambhu, M. (2022). Design and fabrication of solar dryer system for food preservation of vegetables or fruit. *Journal of Food Quality*, 68, 455-461.
18. Xi, H.; Liu, Y.; Guo, L.; and Hu, R. (2020). Effect of ultrasonic power on drying process and quality properties of far-infrared radiation drying on potato slices. *Food Science and Biotechnology*, 29(1), 93-101.
19. Hii, C.L.; Law, C.L.; and Cloke, M. (2008). Modelling of thin layer drying kinetics of cocoa beans during artificial and natural drying. *Journal of Engineering Science and Technology* (*JESTEC*), 3(1), 1-10.
20. Kumar, N.; Sarkar, B.C.; and Sharma, H.K. (2011). Effect of air velocity on kinetics of thin layer carrot pomace drying. *Food Science and Technology International*, 17(5), 459-469.
21. Deshmukh, A.W.; Varma, M.N.; Yoo, C.K.; and Wasewar, K.L. (2014). Investigation of solar drying of ginger (*Zingiber officinale*): Emprical modelling, drying characteristics, and quality study. *Chinese Journal of Engineering*, 2014, 1-7.
22. Guo, H.-L.; Chen, Y.; Xu, W.; Xu, M.-T.; Sun, Y.; Wang, X.-C.; Wang, X.-Y.; Luo, J.; Zhang, H.; and Xiong, Y.-K. (2022). Assessment of drying

kinetics, textural and aroma attributes of Mentha haplocalyx leaves during the hot air thin-layer drying process. *Foods*, 11(6), 784.

23. Shalini, J.S.; Samsher, S.C.; Vivak K.; Neelesh C.; and Manoj, K.Y. (2017). Effect of moisture content and drying rate on dried aonla shreds during ambient storage. *International Journal of Chemical Studies*, 5(4), 362-366.
24. Hii, C.L.; Law, C.L.; Cloke, M.; and Suzannah, S. (2009). Thin layer drying kinetics of cocoa and product quality. *Biosystems Engineering*, 102(2), 153-161.
25. Crank, J. (1979). *The mathematics of diffusion*. Oxford University Press.
26. Taheri-Garavand, A.; Rafiee, S.; and Keyhani, A. (2011). Study on effective moisture diffusivity, activation energy and mathematical modeling of thin layer drying kinetics of bell pepper. *Australian Journal of Crop Science*, 5(2), 128-131.
27. Senadeera, W.; Adiletta, G.; Önal, B.; Di Matteo, M.; and Russo, P. (2020). Influence of different hot air drying temperatures on drying kinetics, shrinkage, and colour of persimmon slices. *Foods*, 9(1), 101.
28. Guiné, R.P.F.; and Barroca, M.J. (2011). Effect of drying on the textural attributes of bell pepper and pumpkin. *Drying Technology*, 29(16), 1911-1919.
29. Thai Community Product Standard. (2015). Dried fruits and vegetables. Retrieved May 1, 2022, from https://tcps.tisi.go.th
30. Dryden, I.G.C. (1982). *Chapter 9 - Drying, conditioning and industrial space heating*. The Efficient use of energy (2nd ed.), Butterworth-Heinemann, 166-198.
31. Madamba, P.S.; Driscoll, R.H.; and Bruckle, K.A. (1996) The thin-layer drying characteristics of garlic slices. *Journal of Food Engineering*, 29, 75-97.
32. Ignacio, L.C.; Irineo, L.L.C.; Marcus, N.; Busarakorn, M.; and Joachim, M. (2018). Thin layer drying of pineapple (*Ananas comosus* L.). *Ingeniería Investigación y Tecnología*, 19(3), 329-342.
33. Babatunde, T.O.; Oseni, K.; and Taiwo, R.B. (2017). Modelling of thin-layer drying characteristic of unripe Cardaba banana (*Musa* ABB) slices. *Cogent Food & Agriculture*, 3(1), 1-12.
34. Guiné, R.P.F.; and Barroca, M.J. (2012). Effect of drying treatments on texture and color of vegetables (pumpkin and green pepper). *Food and Bioproducts Processing*, 90(1), 58-63.
35. Deng, L.Z.; Yang, X.H.; Mujumdar, A.S.; Zhao, J.H.; Wang, D.; Zhang, Q.; Wang, J.; Gao, Z.; and Xiao, H. (2018). Red pepper (*Capsicum annuum* L.) drying: Effects of different drying methods on drying kinetics, physicochemical properties, antioxidant capacity, and microstructure. *Drying Technology*, 36(8), 893-907.
36. Özkan-Karabacak, A.; Özcan-Sinir, G.; Çopur, A.E.; and Bayizit, M. (2022). Effect of osmotic dehydration pretreatment on the drying characteristics and quality properties of semi-dried (intermediate) kumquat (*Citrus japonica*) slices by vacuum dryer. *Foods*, 11(14), 2139.
37. Chauhan, O.P.; Ajai, S.; Asha, S.; Raju, P.S.; and Bawa, A.S. (2011). Effects of osmotic agents on colour, textural, structural, thermal, and sensory properties of apple slices. *International Journal of Food Properties*, 14, 1037-1048.